Electronic structure of the N-*V* center in diamond: Theory

A. Lenef* and S. C. Rand
Division of Applied Physics, 1049 Randall Laboratory, University of Michigan, Ann Arbor, Michigan 48109-1120
(Received 4 August 1995)

Ab initio calculations have been made of possible excited electronic structure of the N-*V* center in diamond. Molecular-orbital basis states for a center of C_{3v} symmetry with $n=2$, 4, or 6 active electrons, which account fully for spin symmetries of the wave functions, were constructed to permit predictions of level structures, degeneracies, and splitting patterns under the action of several magnetic and nonmagnetic interactions. Detailed predictions of the resulting three models taking spin-orbit, spin-spin, strain, and Jahn-Teller interactions into account are given in the form of term diagrams.

I. INTRODUCTION

The N-*V* center in diamond is known to consist of a nitrogen atom and a first-neighbor vacancy in the carbon lattice.[1–4] The picture of unsatisfied bonds at the center, therefore, includes three dangling bonds on the carbon atoms bordering the vacancy and two bonding electrons on the nitrogen atom, for a total of five electrons. Electron-paramagnetic-resonance (EPR) (Refs. 5–7) and hole-burning (Refs. 8–10) experiments have revealed, however, that the ground state is a spin triplet, implying that the number of active electrons at the center is even, in apparent contradiction with this picture. It is the purpose of the present paper to try to resolve this discrepancy and provide a basis for calculating the excited-state structure observed recently by photon echo techniques,[11] in this fundamental defect of diamond.

Analysis of hyperfine splittings and EPR intensities[3,12] indicates that coupling of active electrons to nitrogen is weaker in the N-*V* center than coupling to carbons adjacent to the vacancy. This suggests that active electrons concentrate near these carbons, but does not reveal their number. The existence of triplet levels originally prompted Loubser and van Wyk[3] to suggest that the center captures an extra electron to form a six-electron center. The center would consequently acquire a negative charge in this model. However, this conclusion runs counter to the observed lack of volatility among the active electrons of the center. The N-*V* center is stable up to temperatures at which even the very massive nitrogen atoms themselves become mobile.[4] Comparing this with the ease of ionization of excess electron centers in alkali halides,[13] it is hard to understand how a shallow electron trap could exhibit such exceptional stability.

As a point of departure to resolve this puzzling situation, we have calculated multielectron wave functions for N-*V* models containing $n=2$, 4, and 6 active electrons. By properly accounting for point symmetry and spin properties in these multielectron models, it is possible to order the energy states and calculate perturbation matrix elements for various interactions important within the center. The interactions considered included spin-orbit, spin-spin, strain, and Jahn-Teller interactions. Term diagrams are given, which summarize the predicted electronic structure for each model.

An important finding, which emerges from this work when compared with experiment, is that only the two active electrons associated with the nitrogen atom seem to be necessary to understand the origin of observed electronic states, optical transitions, and stability of the center. The dangling bonds on carbons adjacent to the vacancy are apparently inactive, apart from a possible role in persistent hole-burning within this center.[10] We are thus led to conclude that the N-*V* center is a neutral rather than a negatively charged nitrogen-vacancy center with properties dominated by its two unpaired nitrogen electrons. In the ground state, these two electrons are permitted to be unpaired, because of the presence of the vacancy. Optical excitations on the zero-phonon line at 1.945 eV are well-described by transitions of the electron, which penetrates the vacancy deeply, when a dynamic Jahn-Teller interaction in the excited E state is taken into account.

II. WAVE FUNCTIONS

A. One-electron orbitals

The application of molecular-orbital (MO) techniques to construct wave functions for defect centers in diamond was first performed by Coulson and Kearsley,[14] who applied linear combinations of atomic orbitals (LCAO) to the neutral vacancy. Subsequently, Loubser and van Wyk[3] proposed a MO-LCAO model of the N-*V* center, based on the expectation that all dangling bonds at the vacancy were active, together with two electrons from the nitrogen and a sixth electron trapped by the center to render the total number even. This model is able to account for the existence of triplet states. However, it predicts a singlet ground state, in disagreement with current experiments. In this section, we give a systematic consideration to models based on $n=2$, 4, and 6 active electrons, in which many-electron states are properly symmetrized and ordered energetically to explore the theoretical structure of this center further.

The basic physical structure and geometry of the N-*V* center is shown in Fig. 1. In the present work, single-electron molecular orbitals were built up from linear combinations of one nitrogen sp^3 orbital and three tetrahedrally coordinated sp^3 carbon orbitals dangling in the vacancy (Fig. 1). The carbon atomic orbitals were labeled a, b, and c and the nitrogen orbital d. Molecular orbitals with C_{3v} symmetry were then constructed as orthonormal, real linear combinations of the atomic orbitals a, b, c, and d, using projection operator techniques:[15]

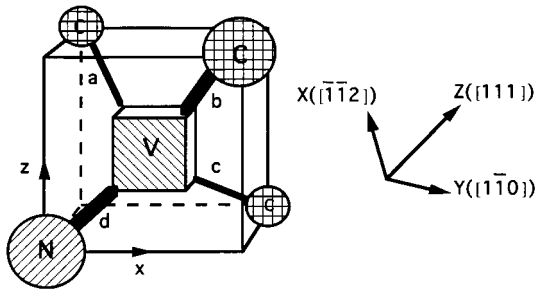

FIG. 1. Physical structure of the N-V center, consisting of a substitutional nitrogen impurity (N) adjacent to a carbon vacancy (V). Both constituents are tetrahedrally coordinated to one another and three carbon atoms (C). Bond directions for molecular orbitals of the center are labeled a, b, c, and d and two Cartesian reference frames are distinguished: the crystal coordinate frame x, y, z (aligned with crystallographic directions) and the defect coordinate frame X, Y, and Z.

$$u = d - \lambda \nu, \tag{1}$$

$$\nu = (a+b+c)/\sqrt{3+6S}, \tag{2}$$

$$e_X = (2c-a-b)/\sqrt{6-6S}, \tag{3}$$

$$e_Y = (a-b)/\sqrt{2-2S}. \tag{4}$$

Functions (1) and (2) transform as A_1 representations (or as Z), whereas functions (3) and (4) transform as E_X and E_Y representations (as X and Y, respectively). λ and S are overlap integrals defined by

$$S = \int (ab)\, d\tau \tag{5}$$

and

$$\lambda = \int (d\nu)\, d\tau. \tag{6}$$

Symmetry and charge considerations can be applied to order these one-electron orbitals energetically. The u orbital should have the lowest energy, being localized on the highly polarized nitrogen. The next lowest orbital should be the ν orbital, since it is totally symmetric. High-symmetry orbitals like ν tend to localize between nuclei of aggregate centers, where they enjoy the attraction of two or more nuclei.[15] Lower-symmetry orbitals tend to have nodes between adjacent nuclei, which raise their energy. Doubly degenerate e orbitals should have the highest energy among the basis states.

B. Multielectron orbitals

For calculations with more than one electron, we assume that total spin is a good quantum number, in accord with early experiments.[3] We proceed to find spin eigenstates, implicitly taking advantage of the fact that total spin commutes with permutation, and then generate total wave functions with the correct irreducible orbital angular momentum representations, analogous to the procedure for weak L-S coupling in simple atoms. Hence, the first step is to take appropriate linear combinations of Slater determinants formed with the one-electron molecular orbitals in (1)–(4).

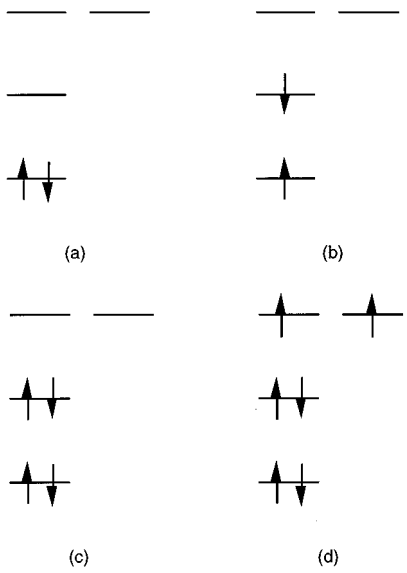

FIG. 2. Possible ground-state spin configurations for various models of the N-V center, having different numbers n of active electrons. (a), (b) $n=2$. (c) $n=4$. (d) $n=6$.

In the ground-state configuration, orbitals are filled according to the Pauli exclusion principle and Hund's rules. Symmetry is determined by examining the direct product of occupied one-electron orbitals. Since the number of active electrons in the N-V center is not known presently, we have calculated three cases, with $n=2$, 4, and 6 electrons. All three cases are consistent with the requirement for an even number of active electrons, necessary to generate triplet states.[3,5–7] The $n=4$ and 6 cases correspond to the charged centers $(\text{N-}V)^+$ and $(\text{N-}V)^-$, respectively. The $n=2$ case corresponds to a physical situation in which two electrons (from the nitrogen) dominate the electromagnetic response. This requires the three unpaired carbon electrons to retract away from the center in such a way that they do not contribute importantly to magnetic or optical properties.

For $n=2$, the expected ground-state configuration is the spin singlet state u^2 with $A_1 \otimes A_1 = A_1$ symmetry (both u and ν are totally symmetric singlets). Because of large Coulomb repulsion between electrons in the same orbital, it is possible that a $u\nu$ configuration might achieve lower energy. Reduction of electron-electron repulsion in a $u\nu$ configuration could potentially offset any increase in electron-core interaction energy. Hence both possible configurations are shown schematically in Figs. 2(a) and 2(b). Note that the $u\nu$ configuration may be either singlet or triplet.

For $n=4$, the expected configuration of the ground state is $u^2\nu^2$. This multielectron molecular orbital achieves a closed core configuration, and is a singlet. Its symmetry is $A_1 \otimes A_1 \otimes A_1 \otimes A_1 = A_1$. This state is represented in Fig. 2(c).

For $n=6$, the ground-state configuration should be given by $u^2\nu^2e^2$. This model has a closed $u^2\nu^2$ core with A_1 symmetry and zero total spin. The remaining two electrons are permitted to be in different e orbitals, so that the spin configuration could, in principle, be either singlet or triplet. However, according to Hund's first rule,[15] the ground state

TABLE I. Irreducible representations of the group C_{3v}.

C_{3v}	E	C_3	C_3'	σ_{va}	σ_{vb}	σ_{vc}
A_1	1	1	1	1	1	1
A_2	1	1	1	-1	-1	-1
E	$\begin{pmatrix} 1 & 0 \\ 0 & 1 \end{pmatrix}$	$\begin{pmatrix} -\frac{1}{2} & \frac{\sqrt{3}}{2} \\ -\frac{\sqrt{3}}{2} & -\frac{1}{2} \end{pmatrix}$	$\begin{pmatrix} -\frac{1}{2} & -\frac{\sqrt{3}}{2} \\ \frac{\sqrt{3}}{2} & -\frac{1}{2} \end{pmatrix}$	$\begin{pmatrix} 1 & 0 \\ 0 & -1 \end{pmatrix}$	$\begin{pmatrix} -\frac{1}{2} & -\frac{\sqrt{3}}{2} \\ -\frac{\sqrt{3}}{2} & \frac{1}{2} \end{pmatrix}$	$\begin{pmatrix} -\frac{1}{2} & \frac{\sqrt{3}}{2} \\ \frac{\sqrt{3}}{2} & \frac{1}{2} \end{pmatrix}$

adopts the highest value of S consistent with the Pauli exclusion principle. To satisfy the requirement that the total wave function be antisymmetric, the electronic part must be of the form $e_X e_Y$ and the ground-state molecular orbital must be the spin triplet $u^2\nu^2 e_X e_Y$; illustrated in Fig. 2(d).

1. Spin eigenstates

To predict interactions within the N-V center, which take spin and orbital degrees of freedom into account, multielectron states with well-defined total spin and orbital angular momentum need to be determined. These may be generated from linear combinations of Slater determinants based on single-electron molecular orbitals and may again be ordered according to increasing energy. Eigenstates of total spin S are formed first, using functions which include spin and real-space coordinates. Then product state representations with the appropriate transformation properties for both spin and orbital angular momentum, which are irreducible with respect to the real-space point group of the center, can be constructed (Sec. II B 2) to obtain total wave functions of the multielectron system with the correct spatial symmetry (see Table I). In this way, the tedious intermediate step of explicit construction of orbital angular momentum eigenstates can be avoided.

To simplify the notation, Slater determinants are written in the form $|ab\ldots r\rangle$, defined by

$$|a\overline{b}\cdots r\rangle = \frac{1}{\sqrt{N!}}\begin{vmatrix} a(1)\alpha(1) & a(2)\alpha(2) & \cdots & a(N)\alpha(N) \\ b(1)\beta(1) & b(2)\beta(2) & \cdots & b(N)\beta(N) \\ \vdots & \vdots & & \vdots \\ r(1)\alpha(1) & r(2)\alpha(2) & \cdots & r(N)\alpha(N) \end{vmatrix}$$

$$= \frac{1}{\sqrt{N!}}\sum_P (-1)^{\Theta(P)} \times [a(1)\alpha(1)b(2)\beta(2)\cdots r(N)\alpha(N)]_P . \quad (7)$$

The labels $a,b\ldots r$ refer to electronic orbitals, which depend on real-space variables, while α and β are one-electron spin-up and spin-down basis states, respectively. P is the permutation operator over the N electrons. The overbar designates spin-down states. The function $\Theta(P)$ is defined by

$$\Theta(P) = \begin{cases} 1, & P \text{ is odd permutation} \\ 0, & P \text{ is even permutation.} \end{cases}$$

In n-electron models, these symmetrized states belong to various configurations of the form $u^l\nu^m e^p$, where the number of active electrons in the center is $n=l+m+p$. For the purposes of this paper l, m, and p are the integers 0, 1, 2, or 3 and $n=2$, 4, or 6.

For $n=2$, the lowest-energy configurations are u^2, ν^2, and $u\nu$. Since these states are all orbital singlets, which have A_1 symmetry, only a spin-singlet, two-electron state can satisfy the Pauli principle in the u^2 configuration. This state is given by

$$|u\overline{u}\rangle = 1/\sqrt{2}[u(1)\overline{u}(2) - u(2)\overline{u}(1)]. \quad (8)$$

A similar result applies to the ν^2 configuration. The $u\nu$ configuration is spanned by the Slater states $|u\nu\rangle$, $|\overline{u\nu}\rangle$, $|u\overline{\nu}\rangle$, and $|\overline{u\nu}\rangle$, which can be combined into the singlet $[|\overline{u\nu}\rangle - |u\overline{\nu}\rangle]/\sqrt{2}$ and the triplet states $|u\nu\rangle$, $[|\overline{u\nu}\rangle + |u\overline{\nu}\rangle]/\sqrt{2}$, and $|\overline{u\nu}\rangle$, in accord with the familiar spin-up and spin-down combinations $\alpha\alpha$, $(\alpha\beta+\beta\alpha)/\sqrt{2}$, and $\beta\beta$.

The configurations next lowest in energy are the ue and νe, which transform as $A_1\otimes E = E$ in real space. The allowable Slater states, in this case, are $|ue_X\rangle$, $|\overline{ue}_X\rangle$, $|u\overline{e}_X\rangle$, $|\overline{ue}_X\rangle$, $|ue_Y\rangle$, $|\overline{ue}_Y\rangle$, $|u\overline{e}_Y\rangle$, and $|\overline{ue}_Y\rangle$. These can easily be combined as above into singlets and triplets.

In the e^2 configuration, the basis set transforms as $E\otimes E = A_1\oplus A_2\oplus E$. Indistinguishability of the particles reduces the sixteen possible states (four spin and four accessible orbital angular momentum states) of this configuration to six linearly independent Slater states: $|e_X\overline{e}_X\rangle$, $|e_Y\overline{e}_Y\rangle$, $|e_X e_Y\rangle$, $|\overline{e}_X\overline{e}_Y\rangle$, $|e_X\overline{e}_Y\rangle$, and $|\overline{e}_X e_Y\rangle$. Multielectron eigenstates in the spin variables can, therefore, be constructed by taking appropriate linear combinations of these Slater basis states as shown below.

States in which the two electrons have the same orbital angular momentum are necessarily singlet, whereas states involving different orbitals may be either singlet or triplet. However, these states are completely analogous to those of u^2 when the two electrons occupy the same orbital and to $u\nu$ when they occupy different orbitals. Hence, with the notational replacements $u\overline{u}\rightarrow e_i\overline{e}_i$ and $u\nu\rightarrow e_X e_Y$, we can write down the singlets directly,

$$\frac{1}{\sqrt{2}}[|e_X\overline{e}_X\rangle + |e_Y\overline{e}_Y\rangle],\ \frac{1}{\sqrt{2}}[|\overline{e}_X e_Y\rangle - |e_X\overline{e}_Y\rangle],$$

TABLE II. Spin wave functions for the N-V center ($n=2$), in the notation of Eq. (7). Only wave functions with the highest value of spin projection ($m_s=S$) are listed. Symmetry of each state is given as Γ and its degeneracy is tabulated under g. E symmetry wave functions are listed in pairs, with the first transforming as x and the second as y.

Configuration	Γ	g	Wave function ($m=S$)
u^2	$^1A_1$	1	$\lvert u\overline{u}\rangle$
ν^2	$^1A_1$	1	$\lvert \nu\overline{\nu}\rangle$
$u\nu$	$^1A_1$	1	$\lvert u\overline{\nu}\rangle-\lvert \overline{u}\nu\rangle$
	$^3A_1$	3	$\lvert u\nu\rangle$
ue	^1E	2	$\lvert u\overline{e_X}\rangle-\lvert \overline{u}e_X\rangle, \lvert ue_Y\rangle-\lvert \overline{u}e_Y\rangle$
	^3E	6	$\lvert ue_X\rangle, \lvert ue_Y\rangle$
νe	^1E	2	$\lvert \nu\overline{e_X}\rangle-\lvert \overline{\nu}e_X\rangle, \lvert \nu\overline{e_Y}\rangle-\lvert \overline{\nu}e_Y\rangle$
	^3E	6	$\lvert \nu e_X\rangle, \lvert \nu e_Y\rangle$
e^2	$^1A_1$	1	$\lvert e_X\overline{e_X}\rangle+\lvert e_Y\overline{e_Y}\rangle$
	$^3A_2$	3	$\lvert e_Xe_Y\rangle$
	^1E	2	$\lvert e_X\overline{e_X}\rangle-\lvert e_Y\overline{e_Y}\rangle$, $\lvert \overline{e_X}e_Y\rangle-\lvert e_X\overline{e_Y}\rangle$

$$\frac{1}{\sqrt{2}}\left[\lvert e_X\overline{e_X}\rangle-\lvert e_Y\overline{e_Y}\rangle\right].$$

In the present basis, the triplet states are similarly found to be

$$\lvert e_Xe_Y\rangle,\ \frac{1}{\sqrt{2}}\left[\lvert \overline{e_X}e_Y\rangle+\lvert e_X\overline{e_Y}\rangle\right],\ \lvert \overline{e_Xe_Y}\rangle.$$

These states and those for other configurations of the two-electron model are listed together in Table II.

For $n=4$, the highest symmetry configuration is the singlet $u^2\nu^2$. The next highest configurations are the $u^2\nu e$ and the $u\nu^2e$, which are equivalent to the $n=2$ configurations ue and νe, because u^2 and ν^2 form closed cores. The corresponding spin basis states have the form $\lvert u\overline{u}\nu e\rangle$ and $\lvert \nu\overline{\nu}ue\rangle$ and occur in combinations identical to those for ue and νe in Table II. The same is true for u^2e^2 and ν^2e^2, which give results identical to the e^2 configuration.

The $u\nu e^2$ configuration contains quintet states. As for the e^2 configuration, the product space transforms as $A_1\oplus A_2\oplus E$, but it is useful to distinguish states that transform as XY from those that transform as XX or YY, since only XY states can have A_1 symmetry. In all there are 24 possible states, when one accounts for the four independent spin orientations of the $u\nu$ orbitals among the six orbital kets $\lvert u\nu e_Xe_Y\rangle$, $\lvert u\nu e_X\overline{e_Y}\rangle$, $\lvert u\nu \overline{e_X}e_Y\rangle$, $\lvert u\nu \overline{e_Xe_Y}\rangle$, $\lvert u\nu e_X\overline{e_X}\rangle$, and $\lvert u\nu e_Ye_Y\rangle$.

To construct four-particle wave functions of well-defined spin, the direct product of four-electron states may be decomposed first into irreducible representations according to

$$[D^{1/2}]^4=(D^1\oplus D^0)\otimes(D^1\oplus D^0)=2D^0+3D^1+D^2. \quad (9)$$

The intermediate decomposition in (9) contains the terms $D^1\otimes D^1$, $D^1\otimes D^0$, $D^0\otimes D^1$, and $D^0\otimes D^0$, which may be written down easily in terms of two-particle spin states. A shorthand notation for these two-particle states, which ignores orbital labels, is expedient, representing the two-particle singlet as $(\alpha\beta-\beta\alpha)/\sqrt{2}$ and the triplet states as $\alpha\alpha$, $(\alpha\beta+\beta\alpha)/\sqrt{2}$, and $\beta\beta$. Use of this notation will necessitate the replacement of spin states α and β by the corresponding configuration labels u, ν, e and their overbar counterparts at the end of the calculation. However, using these two-particle states to form the necessary products, we can immediately write the four-particle singlet $D^0\otimes D^0$ as

$$\Psi(0,0;S=0,m_s=0)\leftrightarrow\tfrac{1}{2}(\alpha\beta\alpha\beta-\alpha\beta\beta\alpha-\beta\alpha\alpha\beta+\beta\alpha\beta\alpha). \quad (10a)$$

The arguments of the wave function $\Psi(S_1,S_2;S,m_s)$, in this case, specify the two spins S_1 and S_2, which span the product space of total spin S and its projection m_s on the axis of quantization. The $D^1\otimes D^0$ and $D^0\otimes D^1$ products yield six of the nine triplets for this four-electron configuration,

$$\Psi(1,0;S=1,m_s=1)\leftrightarrow\frac{1}{\sqrt{2}}(\alpha\alpha\alpha\beta-\alpha\alpha\beta\alpha), \quad (10b)$$

$$\Psi(1,0;S=1,m_s=0)\leftrightarrow\frac{1}{2}(\alpha\beta\alpha\beta-\alpha\beta\beta\alpha+\beta\alpha\alpha\beta-\beta\alpha\beta\alpha), \quad (10c)$$

$$\Psi(1,0;S=1,m_s=-1)\leftrightarrow\frac{1}{\sqrt{2}}(\beta\beta\alpha\beta-\beta\beta\beta\alpha), \quad (10d)$$

$$\Psi(0,1;S=1,m_s=1)\leftrightarrow\frac{1}{\sqrt{2}}(\alpha\beta\alpha\alpha-\beta\alpha\alpha\alpha), \quad (10e)$$

$$\Psi(0,1;S=1,m_s=0)\leftrightarrow\frac{1}{2}(\alpha\beta\alpha\beta+\alpha\beta\beta\alpha-\beta\alpha\alpha\beta-\beta\alpha\beta\alpha), \quad (10f)$$

$$\Psi(0,1;S=1,m_s=-1)\leftrightarrow\frac{1}{\sqrt{2}}(\alpha\beta\beta\beta-\beta\alpha\beta\beta). \quad (10g)$$

The remaining singlet, three more triplets, and quintet states are all derived from the $D^1\otimes D^1$ product. The singlet is

$$\Psi(1,1;S=0,m_s=0)\leftrightarrow 1/2\sqrt{3}(2\alpha\alpha\beta\beta-\alpha\beta\alpha\beta-\alpha\beta\beta\alpha-\beta\alpha\alpha\beta-\beta\alpha\beta\alpha+2\beta\beta\alpha\alpha). \quad (10h)$$

The $m_s=1$ triplet state is

$$\Psi(1,1;S=1,m_s=1)\leftrightarrow\tfrac{1}{2}(\alpha\alpha\alpha\beta+\alpha\alpha\beta\alpha-\alpha\beta\alpha\alpha-\beta\alpha\alpha\alpha), \quad (10i)$$

and the $m_s=2$ quintet state is

$$\Psi(1,1;S=2,m_s=2)\leftrightarrow\alpha\alpha\alpha\alpha. \quad (10j)$$

These and other total wave functions for the lowest-energy configurations of the $n=4$ model are presented in Table III

TABLE III. Spin wave functions for the N-V center ($n=4$), in the notation of Eq. (7). Only wave functions with the highest value of spin projection ($m_s=S$) are listed. E symmetry wave functions are listed in pairs, with the first transforming as x and the second as y.

Configuration	Γ	g	Wave function ($m=S$)
$u^2\nu^2$	$^1A_1$	1	$\lvert u\bar{u}\nu\bar{\nu}\rangle$
$u^2\nu e$	^1E	2	$\lvert u\bar{u}\nu\bar{e}_X\rangle-\lvert u\bar{u}\nu\bar{e}_X\rangle$, $\lvert u\bar{u}\nu\bar{e}_Y\rangle-\lvert u\bar{u}\nu\bar{e}_Y\rangle$
	^3E	6	$\lvert u\bar{u}\nu e_X\rangle$, $\lvert u\bar{u}\nu e_Y\rangle$
$u\nu^3 e$	^1E	2	$\lvert u\nu\bar{\nu}\bar{e}_X\rangle-\lvert\bar{u}\nu\bar{\nu}\bar{e}_X\rangle$, $\lvert u\nu\bar{\nu}\bar{e}_Y\rangle-\lvert\bar{u}\nu\bar{\nu}\bar{e}_Y\rangle$
u^2e^2	$^1A_1$	1	$\lvert u\bar{u}\bar{e}_X\bar{e}_X\rangle+\lvert u\bar{u}\bar{e}_Y\bar{e}_Y\rangle$
	$^3A_2$	3	$\lvert u\bar{u}\bar{e}_X\bar{e}_Y\rangle$
	^1E	2	$\lvert u\bar{u}\bar{e}_X\bar{e}_X\rangle-\lvert u\bar{u}\bar{e}_Y\bar{e}_Y\rangle$, $-[\lvert u\bar{u}\bar{e}_X\bar{e}_Y\rangle-\lvert u\bar{u}\bar{e}_X e_Y\rangle]$
ν^2e^2	$^1A_1$	1	$\lvert\nu\bar{\nu}\bar{e}_X\bar{e}_X\rangle+\lvert\nu\bar{\nu}\bar{e}_Y\bar{e}_Y\rangle$
	$^3A_2$	3	$\lvert\nu\bar{\nu}\bar{e}_X e_Y\rangle$
	^1E	2	$\lvert\nu\bar{\nu}\bar{e}_X\bar{e}_X\rangle-\lvert\nu\bar{\nu}\bar{e}_Y\bar{e}_Y\rangle$, $\lvert\nu\bar{\nu}\bar{e}_X\bar{e}_Y\rangle-\lvert\nu\bar{\nu}\bar{e}_X e_Y\rangle$
$u\nu e^2$	$^1A_1$	1	$\frac{1}{2}[\lvert u\nu\bar{e}_X\bar{e}_X\rangle-\lvert\bar{u}\nu\bar{e}_X\bar{e}_X\rangle+\lvert u\nu\bar{e}_Y\bar{e}_Y\rangle-\lvert\bar{u}\nu\bar{e}_Y\bar{e}_Y\rangle]$
	$^3A_1$	3	$\frac{1}{\sqrt{2}}[\lvert u\nu\bar{e}_X\bar{e}_X\rangle+\lvert u\nu\bar{e}_Y\bar{e}_Y\rangle]$
	$^1A_2$	1	$\frac{1}{2\sqrt{3}}[2\lvert u\nu\bar{e}_X\bar{e}_Y\rangle+2\lvert\bar{u}\nu\bar{e}_X e_Y\rangle-\lvert u\bar{\nu}\bar{e}_X\bar{e}_Y\rangle-\lvert u\bar{\nu}\bar{e}_X e_Y\rangle-\lvert\bar{u}\nu\bar{e}_X e_Y\rangle-\lvert\bar{u}\bar{\nu}\bar{e}_x e_Y\rangle]$
	$^3A_2$	3	$\frac{1}{\sqrt{2}}[\lvert u\bar{\nu}\bar{e}_X e_Y\rangle-\lvert\bar{u}\nu e_X e_Y\rangle]$
	$^3A_2$	3	$\frac{1}{2}[\lvert u\nu e_X\bar{e}_Y\rangle+\lvert u\nu\bar{e}_X e_Y\rangle-\lvert u\bar{\nu}e_X e_Y\rangle-\lvert\bar{u}\nu e_X e_Y\rangle]$
	$^5A_2$	5	$\lvert u\nu e_X e_Y\rangle$
	^1E	2	$\frac{1}{2}[\lvert u\bar{\nu}\bar{e}_X\bar{e}_X\rangle-\lvert\bar{u}\nu\bar{e}_X\bar{e}_X\rangle-\lvert u\bar{\nu}\bar{e}_Y\bar{e}_Y\rangle-\lvert\bar{u}\nu\bar{e}_Y\bar{e}_Y\rangle]$, $\frac{1}{2}[\lvert u\bar{\nu}\bar{e}_X\bar{e}_Y\rangle-\lvert u\bar{\nu}\bar{e}_X e_Y\rangle-\lvert\bar{u}\nu e_X\bar{e}_Y\rangle-\lvert\bar{u}\nu\bar{e}_X e_Y\rangle]$
	^3E	6	$\frac{1}{\sqrt{2}}[\lvert u\nu\bar{e}_X\bar{e}_X\rangle+\lvert u\nu e_Y\bar{e}_Y\rangle]-\frac{1}{\sqrt{2}}[\lvert u\nu e_X\bar{e}_Y\rangle+\lvert u\nu e_Y\bar{e}_X\rangle]$

where the expedient notation of (10) has been replaced by the configurations of (7). As an example, the $^5A_2$ wave function in this table results from (10j), when the four spin labels $\alpha\alpha\alpha\alpha$ are replaced by the ordered sequence of orbital labels $u\nu e_X e_Y$ corresponding to four spin up electrons in the $u\nu e^2$ configuration.

For $n=6$, only the three most symmetric configurations were considered. These are the $u^2\nu^2e^2$, $u^2\nu e^3$, and $u\nu^2e^3$ configurations. The first contains a closed $u^2\nu^2$ core and, therefore, consists of basis states identical to the e^2 configuration of the $n=2$ model. The second and third configurations consist exclusively of ^1E and ^3E states. States with A_1 or A_2 symmetry contain $\bar{e}_X e_X\bar{e}_X$ and $\bar{e}_Y e_Y\bar{e}_Y$ contributions, which violate the Pauli exclusion principle. There are at most two unpaired electrons for these configurations, so that $S=1$ is the maximum value of spin. Spin wave functions for this model are listed in Table IV.

2. Total wave functions

With the multielectron spin eigenstates of Tables II–IV total wave functions spanning the entire direct product space of a given configuration can readily be constructed. In this section, we form linear combinations of the spin eigenstates which transform according to the point group of the center and are therefore irreducible with respect to *both* spin S and orbital angular momentum Ω. This is possible as a result of having chosen a basis of atomic orbitals spanning real space, as well as spin space at the outset.

For $n=2$, the lowest-energy configurations were identified in the last section to be u^2, ν^2, $u\nu$, ue, νe, and e^2. We now form linear combinations of these states to prepare configurational states which are irreducible in C_{3v} symmetry. For a small number of electrons, this is accomplished straightforwardly with the use of the basis function generating machine.[15]

The configurations listed above transform as $A_2\otimes A_2$, $A_1\otimes A_1$, $A_2\otimes A_1$, $A_2\otimes E$, $A_1\otimes E$, and $E\otimes E$, respectively, under C_{3v} point-group symmetry. Product states of the form $\Gamma_i\otimes A_1$ transform as irreducible representations of Γ_i and $A_2\otimes A_2$ transforms as A_1 and $A_2\otimes E$ transforms as E. Many of the product basis states constructed in the last section are, therefore, already acceptable representations of the overall multielectron wave functions, being irreducible with respect to the symmetry group of the center. States constructed from configurations u^2, ν^2, $u\nu$, ue, and νe fall into this category (Table II). The configuration e^2, on the other hand, transforms as $E\otimes E=A_1\oplus A_2\oplus E$. Hence, additional steps are necessary to identify four wave functions which are irreducible in term of S and Ω in this final configuration.

One way to find irreducible total wave functions Ψ is to apply the projection operator[15] to the reducible product of

TABLE IV. Spin wave functions for the N-V center ($n=6$). Only wave functions with the highest value of spin projection ($m_s=S$) are listed. E symmetry wave functions are listed in pairs, with the first transforming as x and the second as y.

Configuration	Γ	g	Wave function ($m=S$)
$u^2\nu^2e^2$	$^1A_1$	1	$\frac{1}{\sqrt{2}}[\lvert u\bar{u}\nu\bar{\nu}e_X\bar{e}_X\rangle+\lvert u\bar{u}\nu\bar{\nu}e_Y\bar{e}_Y\rangle]$
	$^3A_2$	3	$\lvert u\bar{u}\nu\bar{\nu}e_Xe_Y\rangle$
	^1E	2	$\frac{1}{\sqrt{2}}[\lvert u\bar{u}\nu\bar{\nu}e_X\bar{e}_X\rangle-\lvert u\bar{u}\nu\bar{\nu}e_Y\bar{e}_Y\rangle]$,
			$\frac{1}{\sqrt{2}}[\lvert u\bar{u}\nu\bar{\nu}e_X\bar{e}_Y\rangle+\lvert u\bar{u}\nu\bar{\nu}e_Y\bar{e}_X\rangle]$
$u^2\nu e^3$	^1E	2	$\frac{1}{\sqrt{2}}[\lvert u\bar{u}\nu\bar{e}_Xe_Y\bar{e}_Y\rangle-\lvert u\bar{u}\bar{\nu}e_Xe_Y\bar{e}_Y\rangle]$,
			$\frac{1}{\sqrt{2}}[\lvert u\bar{u}\nu\bar{e}_Ye_X\bar{e}_X\rangle-\lvert u\bar{u}\,\bar{\nu}e_Ye_X\bar{e}_X\rangle]$
	^3E	1	$\lvert u\bar{u}\bar{\nu}e_Xe_Y\bar{e}_Y\rangle$, $\lvert u\bar{u}\bar{\nu}e_Ye_X\bar{e}_X\rangle$
$u\nu^2e^3$	^1E	2	$\frac{1}{\sqrt{2}}[\lvert u\nu\bar{\nu}\bar{e}_Xe_Y\bar{e}_Y\rangle-\lvert u\bar{\nu}\nu\bar{e}_Xe_Y\bar{e}_Y\rangle]$,
			$\frac{1}{\sqrt{2}}[\lvert u\nu\bar{\nu}\bar{e}_Ye_X\bar{e}_X\rangle-\lvert u\bar{\nu}\nu\bar{e}_Ye_X\bar{e}_X\rangle]$
	^3E	1	$\lvert u\nu\bar{\nu}\,\bar{e}_Xe_Y\bar{e}_Y\rangle$, $\lvert u\nu\bar{\nu}\,\bar{e}_Ye_X\bar{e}_X\rangle$

two functions Ψ^{Γ_p} and Ψ^{Γ_q}, describing spin and orbital angular momentum portions of the wave function, respectively. The projection operator for the jth representation, denoted by $P^{(j)}$, is defined as

$$P^{(j)}=l_j/h\sum_R \chi^j(R)^*P_R, \tag{11}$$

where l_j is the degree of the representation, h is the number of elements in the group, $\chi(R)$ is the character for operation R, and P_R is the symmetry operation R. As an example, a wave function of A_1 symmetry may be determined in the following way:

$$P^{A_1}(\psi^{E_x}\psi^{E_y})=0,$$

$$P^{A_1}(\psi^{E_x}\psi^{E_x})=\tfrac{1}{2}\,[\psi^{E_x}\psi^{E_x}+\psi^{E_y}\psi^{E_y}]=P^{A_1}(\psi^{E_y}\psi^{E_y}).$$

Applying this procedure to the direct product of the singlet state in (9) and its degenerate counterpart $\lvert e_Y\bar{e}_Y\rangle$, we obtain a total wave function, which transforms as A_1

$$\lvert\Psi^{A_1}\rangle=\frac{1}{\sqrt{2}}\,[\lvert e_X\bar{e}_X\rangle+\lvert e_Y\bar{e}_Y\rangle]. \tag{12a}$$

Similarly, it is easy to show that

$$P^{A_2}(\psi^{E_x}\psi^{E_y})=\tfrac{1}{2}\,[\psi^{E_x}\psi^{E_y}-\psi^{E_y}\psi^{E_x}],$$

$$P^{E_y}(\psi^{E_x}\psi^{E_y})=\tfrac{1}{2}\,[\psi^{E_x}\psi^{E_y}+\psi^{E_y}\psi^{E_x}],$$

and

$$P^{E_x}(\psi^{E_x}\psi^{E_x})=\tfrac{1}{2}\,[\psi^{E_x}\psi^{E_x}-\psi^{E_y}\psi^{E_y}].$$

Taking sign changes due to spin permutation into account, these projections yield the remaining irreducible, total wave functions with A_2, E_x, and E_y symmetries.

$$\lvert\Psi^{A_2}\rangle=\frac{1}{\sqrt{2}}\,[\lvert\bar{e}_Xe_Y\rangle+\lvert e_X\bar{e}_Y\rangle], \tag{12b}$$

$$\lvert\Psi^{E}_X\rangle=\frac{1}{\sqrt{2}}\,[\lvert e_X\bar{e}_X\rangle-\lvert e_Y\bar{e}_Y\rangle], \tag{12c}$$

$$\lvert\Psi^{E}_Y\rangle=-\frac{1}{\sqrt{2}}\,[\lvert e_X\bar{e}_Y\rangle-\lvert\bar{e}_Xe_Y\rangle]. \tag{12d}$$

These states are written in the form $\Psi^{\Gamma_r}_{\alpha}$, where Γ specifies the representation within manifold r (ground or excited state), and α distinguishes X and Y components of the degenerate E representation where applicable.

For $n=4$, the procedure is similar. Only triplet E states, which are degenerate in X and Y, require the construction of linear combinations of the expressions in (10) to be invariant with respect to C_{3v} operations. For example, the appropriate linear combinations of (10b), (10d), and (10i), which yield irreducible total wave functions, are

$$\lvert\Psi^{A_2}\rangle=\Psi(1,1;S=1,m_s=0), \tag{13a}$$

$$\lvert\Psi^{E}_X\rangle=-\frac{i}{\sqrt{2}}\,[\Psi(1,0;S=1,m_s=1)+\Psi(1,0;S=1,m_s=-1)], \tag{13b}$$

$$\lvert\Psi^{E}_Y\rangle=-\frac{1}{\sqrt{2}}\,[\Psi(1,0;S=1,m_s=1)-\Psi(1,0;S=1,m_s=-1)]. \tag{13c}$$

Finally, for $n=6$, we form linear combinations of the $^3A_2$ and ^3E states listed in Table IV. Total wave functions for the ground-state manifold must transform in this case as A_1, E_X, and E_Y of C_{3v},

$$\lvert\Psi^{A_1}\rangle=\frac{1}{\sqrt{2}}\,[\lvert u\bar{u}\nu\bar{\nu}e_X\bar{e}_Y\rangle+\lvert u\bar{u}\nu\bar{\nu}e_Xe_Y\rangle], \tag{14a}$$

$$\lvert\Psi^{E}_X\rangle=\frac{i}{\sqrt{2}}\,[\lvert u\bar{u}\nu\bar{\nu}e_X\bar{e}_Y\rangle-\lvert u\bar{u}\nu\bar{\nu}e_Xe_Y\rangle], \tag{14b}$$

$$\lvert\Psi^{E}_Y\rangle=-\frac{1}{\sqrt{2}}\,[\lvert u\bar{u}\nu\bar{\nu}e_X\bar{e}_Y\rangle-\lvert u\bar{u}\nu\bar{\nu}e_Xe_Y\rangle]. \tag{14c}$$

There are six excited states, which may be written as

$$\lvert(\Psi'_1)^{A_1}\rangle=\frac{1}{\sqrt{2}}\,[\lvert\phi^E_Xv^E_X\rangle+\lvert\phi^E_Yv^E_Y\rangle], \tag{15a}$$

$$\lvert(\Psi'_1)^{A_2}\rangle=\frac{1}{\sqrt{2}}\,[\lvert\phi^E_Xv^E_Y\rangle-\lvert\phi^E_Yv^E_X\rangle], \tag{15b}$$

$$|(\Psi_1')_X^E\rangle = \frac{1}{\sqrt{2}}\,[|\phi_X^E v_X^E\rangle - |\phi_Y^E v_Y^E\rangle], \tag{15c}$$

$$|(\Psi_1')_Y^E\rangle = -\frac{1}{\sqrt{2}}\,[|\phi_X^E v_Y^E\rangle + |\phi_Y^E v_X^E\rangle], \tag{15d}$$

$$|(\Psi_2)_X^E\rangle = -|\phi_Y^E v^{A_2}\rangle, \tag{15e}$$

$$|(\Psi_2')_Y^E\rangle = |\phi_X^E v^{A_2}\rangle, \tag{15f}$$

where

$$|\phi_X^E v^{A_2}\rangle = \frac{1}{\sqrt{2}}\,[|u\bar{u}\nu\bar{e}_X e_Y \bar{e}_Y\rangle + |u\bar{u}\nu\bar{e}_X e_Y \bar{e}_Y\rangle], \tag{16a}$$

$$|\phi_Y^E v^{A_2}\rangle = \frac{1}{\sqrt{2}}\,[|u\bar{u}\nu\bar{e}_Y e_X \bar{e}_X\rangle + |u\bar{u}\nu\bar{e}_Y e_X \bar{e}_X\rangle], \tag{16b}$$

$$|\phi_Y^E v_X^E\rangle = -\frac{i}{\sqrt{2}}\,[|u\bar{u}\nu e_X e_Y \bar{e}_Y\rangle + |u\bar{u}\nu\bar{e}_X e_Y \bar{e}_Y\rangle], \tag{16c}$$

$$|\phi_X^E v_Y^E\rangle = -\frac{1}{\sqrt{2}}\,[|u\bar{u}\nu e_X e_Y \bar{e}_Y\rangle - |u\bar{u}\nu\bar{e}_X e_Y \bar{e}_Y\rangle], \tag{16d}$$

$$|\phi_Y^E v_X^E\rangle = -\frac{i}{\sqrt{2}}\,[|u\bar{u}\nu e_Y e_X \bar{e}_X\rangle + |u\bar{u}\nu\bar{e}_Y e_X \bar{e}_X\rangle], \tag{16e}$$

$$|\phi_Y^E v_Y^E\rangle = -\frac{1}{\sqrt{2}}\,[|u\bar{u}\nu e_Y e_X \bar{e}_X\rangle - |u\bar{u}\nu\bar{e}_Y e_X \bar{e}_X\rangle]. \tag{16f}$$

The product state notation used in (15) and defined explicitly in (16) is discussed in Sec. III A 1.

III. SPIN INTERACTIONS

Using the wave functions of Sec. II, it is possible to predict the energy-level splittings produced by various interactions of electrons within the N-V center. These interactions are specified by the interaction Hamiltonian $H_{\rm int}$ and we consider separately all the main electron interactions for the models introduced above, in order to provide a basis for comparison between theory and experiment. In this section, spin-orbit and spin-spin splittings are calculated. In Secs. IV and V, strain and Jahn-Teller interactions are considered. These calculations are greatly simplified by the availability of eigenstates of the main Hamiltonian, and furnish not only the splittings caused by particular interactions, but also their relative magnitudes.

A. Two-electron model

1. Spin-orbit coupling

We assume that several interactions make important contributions to the fine structure of the N-V center observable by optical and magnetic-resonance methods. First and foremost, we consider the interaction of each electron with its own orbital motion, in this respect, following the treatment of fine structure of atoms. Because of the lack of spherical symmetry of the N-V center, we retain the general form of the relativistic interaction,[16] which can be written as

$$H_{\rm so} = \sum_j \mathbf{\Omega}_j \cdot \mathbf{s}_j\,, \tag{17}$$

in terms of irreducible orbital and spin operators of the jth electron ($j=1,2$). The components of the orbital operator, in the reference frame X, Y, Z of the defect (Fig. 1), are specified by the gradient of the local potential $V(\mathbf{r}_j)$ and the electron momentum $\mathbf{p}_j$,

$$(\Omega_j)_k = 1/2m^2c^2[\nabla V(\mathbf{r}_j)\times\mathbf{p}_j]_k\,. \tag{18}$$

Here, $k=1, 2, 3$ is the spatial component index. According to (18), the orbital components transform as an axial vector. Consequently, direct correspondence between Ω_k and representations of the C_{3v} group can be established:

$$\Omega_X^E = -\Omega_Y\,, \quad \Omega_Y^E = \Omega_X\,, \quad \Omega^{A_2} = \Omega_Z\,.$$

Similarly, transformation properties of the axial spin components for a two-electron system can be verified as

$$S_X^E = -S_Y\,, \quad S_Y^E = S_X\,, \quad S^{A_2} = S_Z\,.$$

The appropriate group-theoretical representation of the spin-orbit Hamiltonian in C_{3v} symmetry, therefore, becomes

$$H_{\rm so} = \sum_j\,[(\Omega^{A_2})_j(S^{A_2})_j + (\Omega_X^E)_j(S_X^E)_j + (\Omega_Y^E)_j(S_Y^E)_j]. \tag{19}$$

The sum is taken over particle number $j=1,2$.

To evaluate spin-orbit matrix elements, we first identify the theoretical manifolds of interest (Table II). We assume that the ground state is the lowest-energy orbital singlet state exhibiting triplet spin and that the state excited by light at 1.945 eV (characteristic of the N-V center) is the lowest-energy doublet with triplet spin. This ensures that the optical transition obeys Laporte's rule and that the spin projection does not change, in agreement with experiments. The ground state is, therefore, expected to be the $^3A_1$ state from the $u\nu$ configuration and the excited state is expected to be the ^3E from the ue configuration.

For convenience in the application of (19), these states may be written out as explicit products of an orbital part ϕ and a spin part v using the results in Table II.

$$\Psi^{A_2} = \phi^{A_1} v^{A_2}, \tag{20a}$$

$$\Psi_X^E = \phi^{A_1} v_X^E\,, \tag{20b}$$

$$\Psi_Y^E = \phi^{A_1} v_Y^E\,, \tag{20c}$$

where

$$\phi^{A_1}=\frac{1}{\sqrt{2}}\,(u\nu-\nu u),$$

and

$$v^{A_2}=v_0,$$

$$v_X^E=-\frac{i}{\sqrt{2}}\,(v_1+v_{-1}),$$

$$v_Y^E=-\frac{1}{\sqrt{2}}\,(v_1-v_{-1}).$$

The spin functions v are conventional rank one spherical tensors. The excited-state manifold, denoted by a prime below, is composed of an orbital doublet wave function and several triplet spin states (six states in all):

$$(\Psi')^{A_1}=\frac{1}{\sqrt{2}}\,(\phi_X^E v_X^E+\phi_Y^E v_Y^E), \tag{21a}$$

$$(\Psi')^{A_2}=\frac{1}{\sqrt{2}}\,(\phi_X^E v_Y^E-\phi_Y^E v_X^E), \tag{21b}$$

$$(\Psi'_1)_X^E=\frac{1}{\sqrt{2}}\,(\phi_X^E v_X^E-\phi_Y^E v_Y^E), \tag{21c}$$

$$(\Psi'_1)_Y^E=\frac{1}{\sqrt{2}}\,(\phi_X^E v_Y^E+\phi_Y^E v_X^E), \tag{21d}$$

$$(\Psi'_2)_X^E=-\phi_Y^E v^{A_2}, \tag{21e}$$

$$(\Psi'_2)_Y^E=\phi_X^E v^{A_2}, \tag{21f}$$

where

$$\phi_X^E=\frac{1}{\sqrt{2}}\,(ue_X-e_Xu),$$

$$\phi_Y^E=\frac{1}{\sqrt{2}}\,(ue_Y-e_Yu).$$

These states can now be used to evaluate spin-orbit interaction matrix elements, providing qualitative and quantitative information on splittings, due to spin-orbit interactions in the $n=2$ model.

Matrix elements are calculated using the spin-orbit Hamiltonian $H_{\rm so}$ of (19). Because $H_{\rm so}$ itself transforms as the identity, only diagonal elements and off-diagonal elements between identical representations of different groups of states are nonzero,

$$\begin{aligned}\langle\Psi_\alpha^{\Gamma_r}|H_{\rm so}|\Psi_\alpha^{\Gamma_s}\rangle&=\sum_{j=1}^{2}\sum_{p,\beta}\langle\Psi_\alpha^{\Gamma_r}|(\Omega_\beta^{\Gamma_p})_j(S_\beta^{\Gamma_p})_j|\Psi_\alpha^{\Gamma_s}\rangle\\&=\sum_{j=1}^{2}\sum_{p,\beta}\sum_{\substack{\gamma,\lambda\\ \gamma',\lambda'}}\begin{pmatrix}k & l\,|\,\Gamma_r\\ \gamma & \lambda\,|\,\alpha\end{pmatrix}^*\begin{pmatrix}k & l\,|\,\Gamma_s\\ \gamma' & \lambda'\,|\,\alpha\end{pmatrix}\langle\phi_\gamma^k|(\Omega_\beta^{\Gamma_p})_j|\phi_{\gamma'}^k\rangle\langle v_\lambda^l|(S_\beta^{\Gamma_p})_j|v_{\lambda'}^l\rangle.\end{aligned} \tag{22}$$

The quantities in large curved parentheses in (22) are Clebsch-Gordon coefficients, describing the decomposition of $|\Psi_\alpha^{\Gamma_r}\rangle$ states in terms of product basis states $|\phi_\gamma^k\rangle|v_\lambda^l\rangle$ (see Appendix). k and l indicate one of the representations (A_1, A_2, E_X, or E_Y) of the space and spin parts of the wave function, respectively. γ, γ', λ, and λ' are indices, which have the value 1 or 2, specifying either X or Y, respectively, for the doubly degenerate representation.

Matrix elements in (22) do not depend on particle number j. Thus, we can introduce total orbital operator $\Omega_\beta^{\Gamma_p}=(\Omega_\beta^{\Gamma_p})_1+(\Omega_\beta^{\Gamma_p})_2$ and spin operator $S_\beta^{\Gamma_p}=(S_\beta^{\Gamma_p})_1+(S_\beta^{\Gamma_p})_2$ to eliminate one summation using the relations $\langle\phi_\gamma^k|\,(\Omega_\beta^{\Gamma_p})_1\,|\phi_{\gamma'}^k\rangle=\langle\phi_\gamma^k|(\Omega_\beta^{\Gamma_p})_2|\phi_{\gamma'}^k\rangle=1/2\langle\phi_\gamma^k|\Omega_\beta^{\Gamma_p}|\phi_{\gamma'}^k\rangle$. Then (22) simply becomes

$$\begin{aligned}\langle\Psi_\alpha^{\Gamma_r}|H_{\rm so}|\Psi_\alpha^{\Gamma_s}\rangle=\tfrac{1}{2}\sum_{p,\beta}\sum_{\substack{\gamma,\lambda\\ \gamma',\lambda'}}&\begin{pmatrix}k & l\,|\,\Gamma_r\\ \gamma & \lambda\,|\,\alpha\end{pmatrix}^*\begin{pmatrix}k & l\,|\,\Gamma_s\\ \gamma' & \lambda'\,|\,\alpha\end{pmatrix}\\&\times\langle\phi_\gamma^k|\Omega_\beta^{\Gamma_p}|\phi_{\gamma'}^k\rangle\langle v_\lambda^l|S_\beta^{\Gamma_p}|v_{\lambda'}^l\rangle.\end{aligned} \tag{23}$$

This relation immediately reveals that all ground-state matrix elements are zero, since Ω transforms as either A_2 or E, and the spatial parts of the wave-function transform as A_1. Neither of the direct products $A_2\otimes A_1\otimes A_1$ or $E\otimes A_1\otimes A_1$ contain the identity. Consequently, there is no first-order spin-orbit splitting of $^3A_1$ in the $n=2$ model.

The situation is different in the excited state. In this case, the orbital matrix elements are of the form $\langle\phi^E|\Omega^{A_2}|\phi^E\rangle$ or $\langle\phi^E|\Omega^E|\phi^E\rangle$, and are permitted to be nonzero by symmetry, since they transform in part as the identity. However, the

wave functions are real and Ω^E is Hermitian and purely imaginary. Consequently, diagonal matrix elements of Ω^E vanish and it may easily be shown that off-diagonal elements are proportional to a reduced, diagonal matrix element which is also zero, using the Wigner-Eckart theorem. The only nonzero terms are matrix elements of Ω^{A_2},

$$-\langle \phi_X^E|\Omega^{A_2}|\phi_Y^E\rangle=\langle \phi_Y^E|\Omega^{A_2}|\phi_X^E\rangle=\langle \phi^E\|\Omega^{A_2}\|\phi^E\rangle. \quad (24)$$

Here, the reduced matrix element $\langle \phi^E\|\Omega^{A_2}\|\phi^E\rangle$ is expressible in terms of a one-electron matrix element as follows.

$$\begin{aligned}\langle \phi^E\|\Omega^{A_2}\|\phi^E\rangle&=\langle \phi_Y^E|\Omega^{A_2}|\phi_X^E\rangle\\&=\langle ue_Y|(\Omega^{A_2})_1|ue_X\rangle+\langle e_Yu|(\Omega^{A_2})_1|e_Xu\rangle\\&=\langle e_Y|(\Omega^{A_2})_1|e_X\rangle. \quad (25)\end{aligned}$$

The last line of (25) makes use of the fact that the one-electron orbital u has A_1 symmetry. The subscript 1 designates the single-particle operator for particle 1.

Matrix elements of the spin operator are handled in the same way. The nonzero contributions are

$$\langle v_X^E|S^{A_2}|v_Y^E\rangle=\langle v_Y^E|S^{A_2}|v_X^E\rangle=\langle v^E\|S^{A_2}\|v^E\rangle, \quad (26a)$$

$$\langle v_X^E|S_X^E|v_X^E\rangle=-\langle v_Y^E|S_X^E|v_Y^E\rangle=\frac{1}{\sqrt{2}}\langle v^E\|S^E\|v^E\rangle, \quad (26b)$$

$$\langle v_X^E|S_Y^E|v_Y^E\rangle=\langle v_Y^E|S_Y^E|v_X^E\rangle=-\frac{1}{\sqrt{2}}\langle v^E\|S^E\|v^E\rangle. \quad (26c)$$

The reduced spin matrix elements yield $\langle v^E\|S^E\|v^E\rangle=\langle v^E\|S^{A_2}\|v^E\rangle=i\hbar$ upon direct evaluation.

With these results, spin-orbit matrix elements for the excited-state manifold can be evaluated. The nonzero elements are

$$\begin{aligned}\langle(\Psi')^{A_1}|H_{\rm so}|(\Psi')^{A_1}\rangle&=-i\frac{\hbar}{2}\langle \phi^E\|\Omega^{A_2}\|\phi^E\rangle\\&=\langle(\Psi')^{A_2}|H_{\rm so}|(\Psi')^{A_2}\rangle\equiv -B, \quad (27a)\end{aligned}$$

$$\langle(\Psi')_X^E|H_{\rm so}|(\Psi')_X^E\rangle=i\frac{\hbar}{2}\langle \phi^E\|\Omega^{A_2}\|\phi^E\rangle\equiv B. \quad (27b)$$

These results are summarized in the middle portion of Fig. 3. For the two-electron model, the excited state is predicted to split into three (doubly degenerate) states with equal separations of magnitude B. The degeneracies that remain are a feature of a multielectron calculation of the states, and arise from the indistinguishability of the electrons.

2. Spin-spin coupling

The usual Hamiltonian governing spin-spin interactions may be written in the form

$$H_{ss}=H'_{ss}+H''_{ss}, \quad (28)$$

where

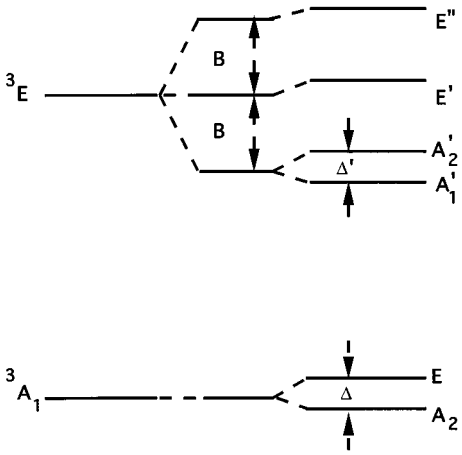

FIG. 3. Schematic diagram of the energy levels predicted for the $n=2$ model of the N-*V* center with no spin interactions (left), spin-orbit interactions only (center), and spin-orbit plus spin-spin interactions (right).

$$H'_{ss}=\frac{1}{2}\frac{g^2\beta^2}{\hbar^2}\sum_{i\neq j}\frac{\mathbf{s}_i\cdot\mathbf{s}_j}{r_{ij}^3}, \quad (29)$$

and

$$H''_{ss}=-\frac{3}{2}\frac{g^2\beta^2}{\hbar^2}\sum_{i\neq j}\frac{(\mathbf{s}_i\cdot\mathbf{r}_i)(\mathbf{s}_j\cdot\mathbf{r}_j)}{r_{ij}^5}. \quad (30)$$

g is the spin g factor, $\beta=e\hbar/2mc$ is the Bohr magneton, and $\mathbf{r}_{ij}$ is the displacement between electrons i and j.

The first term in (28) is a scalar product similar to the one already considered in (19). Hence, it has the form

$$H'_{ss}=\frac{1}{2}\frac{g^2\beta^2}{\hbar^2}\sum_{i\neq j}(S_i^{A_2}S_j^{A_2}+S_{X,i}^ES_{X,j}^E+S_{Y,i}^ES_{Y,j}^E)/r_{ij}^3. \quad (31)$$

The second is given by the irreducible expression

$$\begin{aligned}H''_{ss}=-\frac{3}{2}\frac{g^2\beta^2}{\hbar^2}\sum_{i\neq j}&(T_{ij}^{A_1}W_{ij}^{A_1}+T_{ij}^{A_1'}W_{ij}^{A_1'}-T_{X,ij}^EW_{X,ij}^E\\&-T_{Y,ij}^EW_{Y,ij}^E+T_{X,ij}^{E'}W_{X,ij}^{E'}+T_{Y,ij}^{E'}W_{Y,ij}^{E'}). \quad (32)\end{aligned}$$

Tensors T and W have been introduced to yield an expression in which each separate term transforms as an irreducible bilinear combination of the spatial coordinates. These quantities are defined by

$$\begin{aligned}&T_{ij}^{A_1}=z_{ij}^2/r_{ij}^5, \quad T_{ij}^{A_1'}=\frac{1}{\sqrt{2}}(x_{ij}^2+y_{ij}^2)/r_{ij}^5,\\&T_{X,ij}^E=z_{ij}x_{ij}/r_{ij}^5, \quad T_{X,ij}^{E'}=\frac{1}{\sqrt{2}}(x_{ij}^2-y_{ij}^2)/r_{ij}^5,\\&T_{Y,ij}^E=z_{ij}y_{ij}/r_{ij}^5, \quad T_{Y,ij}^{E'}=-x_{ij}y_{ij}/r_{ij}^5 \quad (33)\end{aligned}$$

and

$$W_{ij}^{A_1}=s_{iz}s_{jz},\quad W_{ij}^{A_1'}=\frac{1}{\sqrt{2}}(s_{ix}s_{jx}+s_{iy}s_{jy}),$$

$$W_{X,ij}^{E}=-(s_{iz}s_{jx}+s_{ix}s_{jz}),\quad W_{X,ij}^{E'}=\frac{1}{\sqrt{2}}(s_{ix}s_{jx}-s_{iy}s_{jy}),$$

$$W_{Y,ij}^{E}=-(s_{iz}s_{jy}+s_{iy}s_{jz}),\quad W_{Y,ij}^{E'}=\frac{1}{\sqrt{2}}(s_{iy}s_{jx}+s_{ix}s_{jy}). \tag{34}$$

In (33) and (34), primed and unprimed tensors merely refer to different combinations of spatial coordinates rather than ground and excited states.

Matrix elements of H_{ss}' are identical for all states in the ground-state manifold of the $n=2$ model. This is an immediate consequence of rewriting the Hamiltonian (29), using the relation $S^2=(S_1+S_2)^2$. This yields

$$H_{ss}'=\frac{g^2\beta^2}{2\hbar^2 r_{12}^3}(S^2-\tfrac{3}{2}), \tag{35}$$

which clearly depends only on total spin S. Hence, first-order H_{ss}' interactions in triplet states of this model are identical, resulting in identical shifts of sublevels without removal of any degeneracy.

Matrix elements of H_{ss}'', on the other hand, depend on position operator r, as well as spin S, and are given by

$$\langle\Psi_\alpha^{\Gamma_r}|H_{ss}''|\Psi_\alpha^{\Gamma_s}\rangle=-3\frac{g^2\beta^2}{\hbar^2}\sum_{p,\beta}\sum_{\substack{\gamma,\lambda\\ \gamma',\lambda'}}\begin{pmatrix}k & l\\ \gamma & \lambda\end{pmatrix}\Big|\begin{matrix}\Gamma_r\\ \alpha\end{matrix}\Big)^*\times\begin{pmatrix}k & l\\ \gamma' & \lambda'\end{pmatrix}\Big|\begin{matrix}\Gamma_s\\ \alpha\end{matrix}\Big)\langle\phi_\gamma^k|T_\beta^{\Gamma_p}|\phi_{\gamma'}^k\rangle\times\langle u_\lambda^l|W_\beta^{\Gamma_p}|u_{\lambda'}^l\rangle. \tag{36}$$

Using the total wave functions of Sec. III A 1 to calculate matrix elements for the A_2 and E symmetry ground states with (36), one obtains a ground-state splitting of

$$\Delta=\langle\Psi^E|H_{ss}|\Psi^E\rangle-\langle\Psi^{A_2}|H_{ss}|\Psi^{A_2}\rangle=\tfrac{3}{2}D_{zz}, \tag{37}$$

where

$$D_{zz}=\tfrac{1}{2}\,g^2\beta^2\left\langle\phi^{A_1}\left|\frac{r_{12}^2-3z_{12}^2}{r_{12}^5}\right|\phi^{A_1}\right\rangle.$$

This is the usual result for spin-spin splitting of an orbitally nondegenerate triplet state in axially symmetric centers.[17] A similar calculation for excited states A_1' and A_2' yields an excited-state splitting Δ' of

$$\Delta'=\langle(\Psi')^{A_2}|H_{ss}|(\Psi')^{A_2}\rangle-\langle(\Psi')^{A_1}|H_{ss}|(\Psi')^{A_1}\rangle=4D_{xy}, \tag{38}$$

where

$$D_{xy}'=\tfrac{1}{2}g^2\beta^2\left\langle\phi_X^E\left|\frac{x_{12}y_{12}}{r_{12}^5}\right|\phi_Y^E\right\rangle.$$

If one neglects overlap between atomic orbitals, the individual splittings Δ and Δ' and their approximate ratio are predicted[18] to be

$$\Delta=\tfrac{3}{4}g^2\beta^2\langle r_{12}^{-3}\rangle(1-3\cos^2\theta), \tag{39a}$$

$$\Delta'=-\tfrac{3}{4}g^2\beta^2\langle r_{12}^{-3}\rangle\sin^2\theta, \tag{39b}$$

$$\frac{\Delta'}{\Delta}=-\frac{\sin^2\theta}{1-3\cos^2\theta}. \tag{39c}$$

To estimate these splittings quantitatively, the angle $\theta=35.3°$ between the symmetry axis z and a line through the centers of the ''a'' and ''d'' orbitals was inserted in (39). The radial integral defined by $\langle r_{12}^{-3}\rangle=\langle da|r_{12}^{-3}|da\rangle$ was estimated using $r_{12}=a_0/\sqrt{2}$, where $a_0=3.56$ Å is the cubic lattice spacing of diamond. The resulting splittings are $\Delta=-2.4$ GHz and $\Delta'=-0.8$ GHz. The energy-level diagram for $n=2$ with spin-orbit and spin-spin interactions is given in Fig. 3.

B. Four-electron model

Basic features of the four-electron model conflict with the observed ground-state structure of the N-V center reported by others. In particular, this model yields a lowest-energy triplet state, with orbital angular momentum of E symmetry (line 3 of Table II). This is contrary to the well-established A character of the ground state.[2,3,5–7] Moreover, no $S=1$ orbital singlet is encountered until one moves up in energy to the fourth configuration u^2e^2. Hence, this model is not considered further in this paper.

C. Six-electron model

1. Spin-orbit coupling

For more than two electrons, calculations of spin-orbit matrix elements become tedious. A second quantization formalism simplifies evaluations by introducing creation and annihilation operators $a_{rs}^\dagger$ and a_{rs} which, respectively, add or subtract one-electron states $|\phi^r|v^s\rangle$ from the total wave function. The Hamiltonian of (19) can be rewritten as

$$H_{\rm so}=\sum_{p,\beta}\sum_{\substack{r,s\\ r's'}}\langle\phi^r|\Omega_\beta^{\Gamma_p}|\phi^{r'}\rangle\langle v^s|S_\beta^{\Gamma_p}|v^{s'}\rangle a_{r's'}^\dagger a_{rs}. \tag{40}$$

The two manifolds of interest theoretically are $^3A_2$ of the $u^2\nu^2e^2$ configuration and ^3E of the $u^2\nu e^3$ configuration in Table IV. In the excited state, only matrix elements of the form (24) give nonzero contributions. Hence on the basis of (25), the spin-orbit interaction Hamiltonian reduces to

$$H_{\rm so}=\tfrac{1}{2}\langle e\|\Omega^{A_2}\|e\rangle(a_{Y\alpha}^\dagger a_{X\alpha}-a_{X\alpha}^\dagger a_{Y\alpha}+a_{X\beta}^\dagger a_{Y\beta}-a_{Y\beta}^\dagger a_{X\beta}). \tag{41}$$

The subscripts X and Y denote e_X and e_Y states, respectively.

With the Hamiltonian of (41), it is readily apparent, even for this multielectron model, that all diagonal matrix elements in the ground-state manifold are zero,

$$\langle\Psi^{A_1}|H_{\rm so}|\Psi^{A_1}\rangle=\langle\Psi_X^E|H_{\rm so}|\Psi_X^E\rangle=\langle\Psi_Y^E|H_{\rm so}|\Psi_Y^E\rangle=0. \tag{42}$$

This is due to the fact that these matrix elements all contain terms similar to

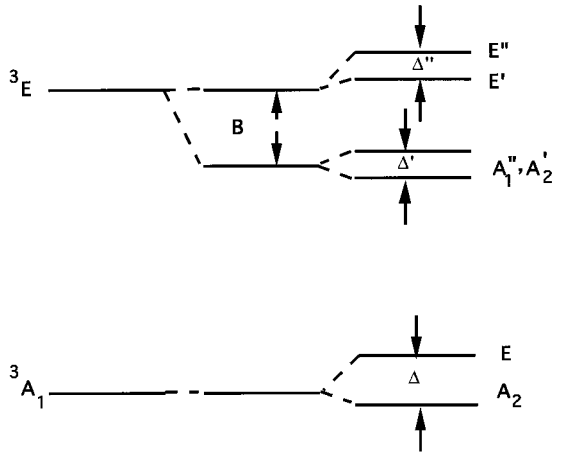

FIG. 4. Schematic diagram of energy levels predicted for the $n=6$ model of the N-V center with no spin interactions (left), spin-orbit interactions only (center), and spin-orbit plus spin-spin interactions (right).

$$\langle u\bar{u}\bar{v}\bar{v}e_X\bar{e}_Y|H_{so}|u\bar{u}\bar{v}\bar{v}e_X\bar{e}_Y\rangle=\langle u\bar{u}\bar{v}\bar{v}e_X\bar{e}_Y|u\bar{u}\bar{v}\bar{v}e_Y\bar{e}_Y\rangle+\langle u\bar{u}\bar{v}\bar{v}e_X\bar{e}_Y|u\bar{u}\bar{v}\bar{v}e_X\bar{e}_X\rangle=0.$$

Off-diagonal terms are zero, because H_{so} transforms as A_1 and the basis states are orthogonal. Hence, the overall matrix element does not transform like the identity. Excited-state matrix elements between E states are also all zero, but between A states they are not.

$$\langle(\Psi')^{A_1}|H_{so}|(\Psi')^{A_1}\rangle=\langle(\Psi')^{A_2}|H_{so}|(\Psi')^{A_2}\rangle=-\frac{i\hbar}{2}\langle e\|(\Omega^{A_2})_1\|e\rangle=-B. \tag{43}$$

Thus, in the $n=6$ model, only A states can shift under the action of spin-orbit interaction, as indicated in Fig. 4.

2. Spin-spin coupling

Qualitative results for the $n=2$ electron model of Fig. 3 apply to the $n=6$ model in Fig. 4. The addition of spin-spin coupling separates A_2 from E by Δ in the ground state, and A_1 from A_2 in the excited state by an amount Δ' much smaller than the spin-orbit splitting B. But the degeneracy of the remaining states is only partially lifted, with E' separating from E'' by Δ''. In the case of six electrons ($n=6$), spin-spin coupling is expected to result in the same number of final states as the $n=2$ model, but magnitudes of the splittings are predicted to be quite different. In particular, the $E'-E''$ splitting should be on the order of the spin-orbit splitting B in the $n=2$ model, but on the order of the spin-spin coupling Δ in the $n=6$ model. These results are presented in Fig. 4.

IV. STRAIN INTERACTIONS

In Sec. III, interactions which did not reduce the point symmetry of the center were calculated. We now treat strain interactions which do cause distortions. The development follows previous work,[2,19] but includes excited-state magnetic interactions.

In irreducible form, the strain Hamiltonian is[21]

$$V=\sum_{i,k} V_{ik}\sigma_{ik}=\frac{V^{A_1}}{\sqrt{3}}(\sigma_{xx}+\sigma_{yy}+\sigma_{zz})+\frac{V_X^E}{\sqrt{6}}(2\sigma_{zz}-\sigma_{xx}-\sigma_{yy})+\frac{V_Y^E}{\sqrt{2}}(\sigma_{xx}-\sigma_{yy}). \tag{44}$$

The strain σ_{ik} and its potential V_{ik} both transform as the second rank coordinate tensor $r_i r_k$ in the crystal coordinate system. The interaction in (44) is written in terms of defect coordinates $\mathbf{R}=(X,Y,Z)$, which relate to the crystal coordinates $\mathbf{r}=(x,y,z)$ of Fig. 1 through the transformation $\mathbf{R}=R\mathbf{r}$, where

$$R=\frac{1}{\sqrt{6}}\begin{pmatrix}-1 & -1 & 2\\ \sqrt{3} & -\sqrt{3} & 0\\ \sqrt{2} & \sqrt{2} & \sqrt{2}\end{pmatrix}. \tag{45}$$

For simplicity, since strains along the defect axis do not reduce the symmetry of the center, we consider only large strains along one of the carbon-vacancy axes and first diagonalize the strain Hamiltonian by itself. The energy of the ^3E state of a center oriented along [111] and subjected to a strain of magnitude σ along [111] acquires two values differing by $E_s=(\sigma/9)\langle\Psi^E\|V^E\|\Psi^E\rangle$. The corresponding eigenstates are

$$|+\rangle=-\frac{1}{2}|\phi_X^E\rangle+\frac{\sqrt{3}}{2}|\phi_Y^E\rangle, \tag{46a}$$

$$|-\rangle=-\frac{\sqrt{3}}{2}|\phi_X^E\rangle-\frac{1}{2}|\phi_Y^E\rangle. \tag{46b}$$

To combine strain and spin-orbit interactions in a two-electron model, the spin-orbit Hamiltonian in (19) is included next, and the problem rediagonalized in the basis of product states $|\pm\rangle|v_{m_s}\rangle$. The new eigenenergies are

$$E^{\pm}=\pm\left(\frac{E_s}{2}\right)\left[1+\left(\frac{2m_sB}{E_s}\right)^2\right]^{1/2}, \tag{47}$$

where B is the spin-orbit parameter defined in Sec. II A 1 and $m_s=1, 0, -1$.

The eigenstates comprising strain and spin-orbit interactions are too cumbersome to reproduce, but calculations with them reveal that when uniaxial strain energy considerably exceeds spin-orbit coupling, the m_s states asymptotically approach the pure $|\pm\rangle$ states of (46) separated by energy E_s. The inclusion of spin-spin interactions removes the remaining degeneracies of $m_s=\pm1$ levels, yielding the term diagram of Fig. 5, in agreement with earlier results.[8]

V. JAHN-TELLER INTERACTIONS

We now consider the dynamic Jahn-Teller (JT) effect which, as is well known,[2,17,20] can also cause a reduction in the symmetry of degenerate states by coupling electronic ex-

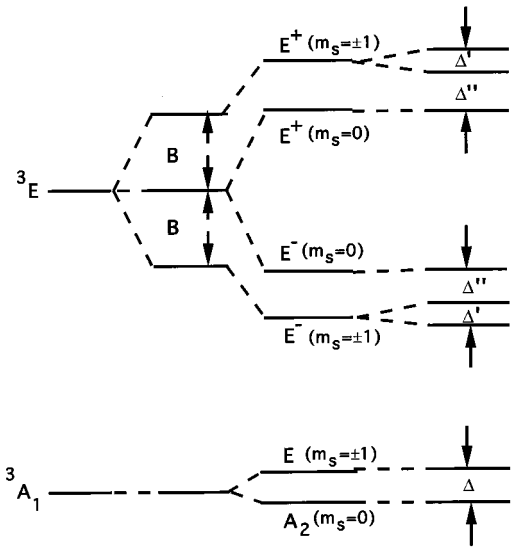

FIG. 5. Schematic diagram of the energy levels predicted for the $n=2$ model of the N-V center with no perturbations (left), spin-orbit interactions only (center left), spin-orbit coupling in the limit of large ⟨111⟩ strain (center right), and spin-orbit with large ⟨111⟩ strain plus the spin-spin interaction (right).

citations to vibrational modes of a lattice. Excited-state interactions were previously investigated experimentally by Davies and Hamer,[2] who explained their observations without invoking JT effects. Here, we nevertheless reexamine JT interactions to see if they can account for newly observed excited-state fine structure.

The Jahn-Teller theorem predicts that degenerate electronic states couple to vibrational modes of like symmetry to achieve spontaneous symmetry breaking, which reduces excitation energy and lifts the degeneracy, unless the degeneracy is of the Kramers type. In the N-V center, the excited E state can, in principle, couple to E vibrational modes of the lattice, causing a dynamic distortion of the excited-state potential with energy minima localized at points of nonzero distortion of the static symmetry group. The resulting *vibronic* wave functions have symmetries determined by the decomposition of the interacting states $E\otimes E=A_1\oplus A_2\oplus E$ and the energy at the dynamic minima on the potential surface is lowered by the Jahn-Teller energy $E_{\rm JT}$.

Two regimes can be differentiated.[17] In the first, the Jahn-Teller energy is smaller than the nuclear zero-point energy associated with the vibrational mode of frequency ω ($E_{\rm JT}\ll\hbar\omega/2$), whereas, in the second, the opposite is true. In the limit of weak JT coupling ($E_{\rm JT}\ll\hbar\omega/2$), the E vibronic state lies below the (degenerate) A_1 and A_2 states and the $E\leftrightarrow A$ separation $\Delta_{\rm JT}$ is somewhat less than a vibrational quantum $\hbar\omega$.[23] In the opposite limit ($E_{\rm JT}\gg\hbar\omega/2$), the splitting between the E and $^3A_1$ level (no longer degenerate with $^3A_2$) may be very much less than a vibrational quantum, and is given by[21]

$$\frac{\Delta_{\rm JT}}{\hbar\omega}=\frac{9\hbar}{8\pi}\left[\frac{2V_3}{E_{\rm JT}}\exp\left(-\frac{3}{2}\frac{\sqrt{E_{\rm JT}V_3}}{\hbar\omega}\right)\right]^{1/2}. \qquad (48)$$

The quantity V_3 in (48) is the cubic strain matrix element of the Jahn-Teller potential.[17] The general situation in the presence of JT coupling is shown in Fig. 6. The $^3A_2$ vibronic state was omitted for simplicity, in view of the fact that electric dipole transitions to this state from the ground state are forbidden with linearly polarized light.

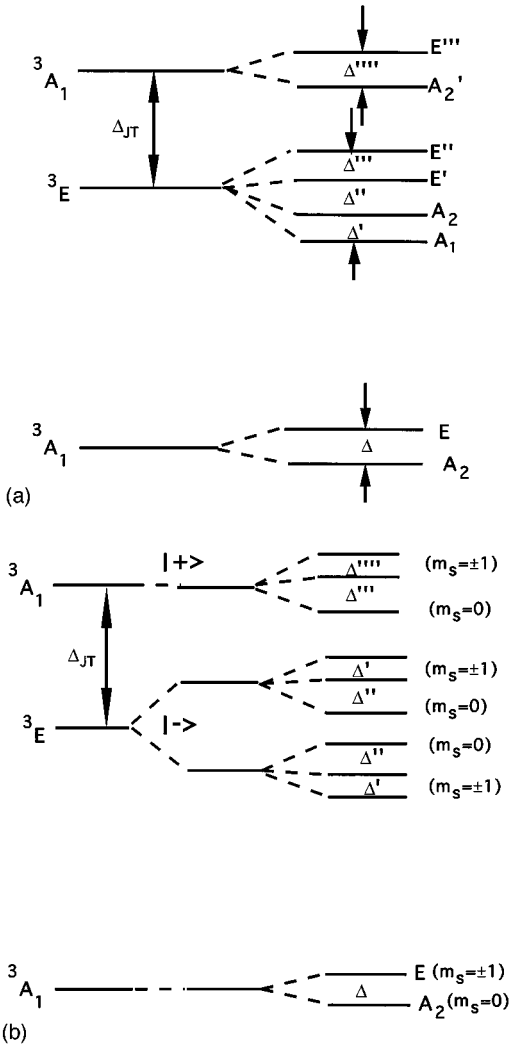

FIG. 6. (a) Schematic diagram of energy levels predicted for the $n=2$ model of the N-V center with a dynamic Jahn-Teller effect in the excited state (left), and with a combination of Jahn-Teller, spin-orbit, and spin-spin interactions (right). (b) Schematic diagram of energy levels predicted for the $n=2$ model of the N-V center with a dynamic Jahn-Teller effect in the excited state (left), the strong-coupling JT limit with random static strain, which splits the excited E *vibronic* state by as much as the inhomogeneous width of the zero-phonon transition (center), and these interactions combined with (residual) spin-orbit and spin-spin interactions (right).

When both V_3 and $E_{\rm JT}$ are large, spin-orbit interactions are *quenched*[17] and the splitting $\Delta_{\rm JT}$ decreases exponentially with increasing $E_{\rm JT}$.[23] Under these conditions, $\Delta_{\rm JT}$ can decrease sufficiently to become comparable to static strain energies within the crystal. Then the static JT interaction causes neighboring wells on the dynamic potential surface created by electron-phonon coupling to acquire significantly different energies. As a result, the degeneracy of the *vibronic* ^3E state splits slightly, as shown in Fig. 6(b). However, the randomness of the static strain contribution to the energy

merely produces a continuous distribution in this splitting of the $|-\rangle$ state, yielding an inhomogeneous width determined by the strain distribution. The strain-dominated diagram to the right of Fig. 5 and the situation in the $|-\rangle$ state of Fig. 6(b) are superficially similar.

With the addition of (partially quenched) spin-orbit and spin-spin interactions, trios of well-defined spin states appear in the electronic structure, as the remaining degeneracies are removed [Fig. 6(b)]. The term diagram including dynamic and static JT effects, spin-orbit and spin-spin interactions [Fig. 6(b)] is distinguished by the presence of the $^3A_1$ state above the excited E state, in addition to the substate trio pattern. The triplet spin splittings within the two parts of the $|-\rangle$ state should be identical, but are expected to differ slightly from those in the excited $^3A_1$ state, due to vibronic interaction. Consequently, there are only two possible (allowed) excited-state radio-frequency rf resonances originating from the ^3E vibronic state and at most two from the $^3A_1$ state lying higher in energy by $\Delta_{\rm JT}$.

VI. DISCUSSION

Figures 3–6 are the main results of this paper. They predict energy-level structures of the N-V center for several multielectron models with various perturbations acting on the defect. Models with two and six electrons have been treated in some detail in this paper, whereas the four-electron model was dismissed in Sec. III B, on the basis of incorrect ground-state structure. Models with odd numbers of electrons were also discarded, since these are inconsistent with the existence of triplet states in the center.[3] Models with two and six active electrons, on the other hand, have correctly ordered $^3A_1$ and ^3E states among low-energy configurations, and at least one intervening metastable state as reported experimentally.[3,7] Both the $n=2$ and 6 models predict complex structure when common excited-state interactions are calculated. However, the relative magnitudes of splittings and the number of final states depend markedly on the number of electrons and the allowed perturbations.

In Fig. 3, it is apparent that the $n=2$ model based purely on spin-orbit and spin-spin interactions yields two large energy splittings in the excited state, but only a single small splitting Δ' on the order of 1 GHz. The $n=6$ model of Fig. 4 predicts two such small splittings Δ' and Δ'' separated by the large spin-orbit energy B. These predictions are both quite different from recent photon echo measurements,[11] in which two rf splittings were reported in an excited triplet lying approximately 46 cm^{-1} below a second excited state with at least one similar fine splitting.

In Fig. 5, it can be seen that static uniaxial strain acting in concert with spin interactions yields an energy-level diagram in better apparent agreement with the experiments in Refs. 8 and 11. However, the emergence of narrow, reproducible energy levels through a uniaxial strain interaction of the type considered in Sec. IV seems unlikely in real diamond crystals for several reasons. Internal strains in crystals typically vary randomly in magnitude and orientation from point to point, and from sample to sample. It is improbable that diamond samples of various origins could have the same dominant uniaxial internal strain. Consequently, it is hard to understand how measurements on many different samples in different laboratories could yield the same results within experimental error.[8–10] Also, no significant shift in rf splitting frequencies has been observed[10] versus the magnitude of internal strain (i.e., position within the inhomogeneously broadened optical transition). Yet ground and excited-state splittings attributed to static strain[19] are vastly different. Moreover, an orientational average of the results given above is really needed to complete the model of Sec. IV, since a fixed uniaxial strain in the crystal frame has different orientations with respect to orientationally distinct centers. But such an average would smear out the effects of strain, since some directions produce no splitting at all. It is, therefore, doubtful that a coarse splitting of the excited state into two parts separated by 46 cm^{-1}, each with reproducible substate splittings as observed experimentally,[8,11,19] occurs by this mechanism.

On the other hand, dynamic Jahn-Teller effects in a two-electron model (Fig. 6) were found to predict results which are both sample independent and are very similar to experiment qualitatively and semiquantitatively. Through vibrational coupling to the lattice, as seen in Fig. 6(a), defect electrons can be promoted to either the ^3E vibronic state or the $^3A_1$ state situated an energy $\Delta_{\rm JT}$ above it. The substate structure depends on whether the effect of static strain is included [Fig. 6(b)] or not [Fig. 6(a)]. More than two rf resonances corresponding to excited-state splittings are expected on the red side of the optical transition when the strain interaction is weaker than both the JT and spin-orbit interactions [Fig. 6(a)]. For a strong JT interaction with random strain intermediate in strength between the dynamic JT and spin interactions, exactly two rf resonances are expected on the red side of the line [Fig. 6(b)]. On the blue side of the line, very rapid vibrational dephasing should cause severe broadening, but at least one rf resonance is expected.

This latter model agrees rather well with photon echo and persistent spectral hole-burning observations. In recent experiments, two rf excited state splittings in rough agreement with the spin-spin coupling estimates of Sec. III A 2 were observed on the red side of the N-V optical resonance.[10,11] A broadened rf resonance was seen at short wavelengths in Ref. 10 and a fast-decaying modulation component observed approximately 46 cm^{-1} to the blue side of the zero-phonon transition in Ref. 11. These observations support only one of the many models considered in this paper, and we conclude that the electronic structure of the N-V center is similar to that given in Fig. 6(b).

The large excited-state splitting observed experimentally[11] can be attributed to a Jahn-Teller interaction, with $\Delta_{\rm JT}=46$ cm^{-1} as shown in Fig. 6(b). This model predicts two broad peaks separated by $\Delta_{\rm JT}$ in the four-wave mixing excitation spectrum. On the red side of the transition, the existence of an inhomogeneous strain distribution in the $|-\rangle$ state (corresponding to the quasistatic Jahn-Teller interaction) should wash out all fine structure other than the Δ' and Δ'' splittings, predicted to be the same for both strain-split components. On the blue side of the transition, at most two splitting frequencies are expected, consistent with four-wave mixing observations.[11]

Earlier analysis attributed depolarization on the optical transition to strain mixing between X and Y components of the ^3E state.[2] As a result, the possibility of Jahn-Teller cou-

pling to E vibrational modes was dismissed. We find that strain indeed plays an important role in excited structure, but obtain better consistency between theory and experiment with a Jahn-Teller interaction picture in which Δ_{JT} is on the order of the inhomogeneous broadening. Consequently, it is concluded that a two-electron model, in which a strong JT effect quenches the spin-orbit interaction, but in which small splittings persist due to spin-spin coupling, can account well for optical experiments to date.[11]

ACKNOWLEDGMENTS

This research was sponsored by the Air Force Office of Scientific Research (H. Schlossberg), and the National Science Foundation Technology Center for Ultrafast Optical Science (STO PHY 8920108). A.L. gratefully acknowledges support from the Department of Education. The authors thank S. W. Brown, T. Hecht, R. Kopelman, and G. W. Ford for helpful discussions.

APPENDIX

Clebsch-Gordan coefficients relate the basis states of a direct product space to explicit products of individual states spanning the lower dimensional component Hilbert spaces. For example, irreducible representations of the total wave function $|\Psi_\alpha^{\Gamma_r}\rangle$ can be expressed in terms of irreducible basis states for orbital angular momentum and spin, given by $|\phi_\gamma^k\rangle$ and $|v_\lambda^l\rangle$, respectively, using expansions of the form

$$|\Psi_\alpha^{\Gamma_r}\rangle=\sum_{\gamma,\lambda}\begin{pmatrix} k & l \\ \gamma & \lambda \end{pmatrix}\begin{matrix} \Gamma_r \\ \alpha \end{matrix}\Big)|\phi_\gamma^k\rangle|v_\lambda^l\rangle. \tag{A1}$$

The symbols $\left(\begin{smallmatrix} k & l \\ \gamma & \lambda \end{smallmatrix}\middle|\begin{smallmatrix} \Gamma_r \\ \alpha \end{smallmatrix}\right)$ are Clebsch-Gordan coefficients of the expansion. They can be evaluated by projection operator techniques and written as unique matrices, apart from an arbitrary phase factor. For C_{3v} symmetry, these coefficients may be obtained quite easily without recourse to the general sum rule that they satisfy.[22] For example, basis-state products of the form $|\phi^k\rangle|v^{A_1}\rangle$ obviously transform as Γ^k. Hence, the Clebsch-Gordan coefficient for this component of $|\Psi^k\rangle$ is the identity. The coefficients for C_{3v} are

$$\begin{pmatrix} A_1 & A_1 \\ 1 & 1 \end{pmatrix}\begin{matrix} A_1 \\ 1 \end{matrix}\Big)=\begin{pmatrix} A_2 & A_1 \\ 1 & 1 \end{pmatrix}\begin{matrix} A_2 \\ 1 \end{matrix}\Big)=\begin{pmatrix} A_1 & A_2 \\ 1 & 1 \end{pmatrix}\begin{matrix} A_2 \\ 1 \end{matrix}\Big) \tag{A2}$$

$$=\begin{pmatrix} A_2 & A_2 \\ 1 & 1 \end{pmatrix}\begin{matrix} A_2 \\ 1 \end{matrix}\Big)=1,$$

$$\begin{pmatrix} E & A_1 \\ i & j \end{pmatrix}\begin{matrix} E \\ k \end{matrix}\Big)=\begin{pmatrix} A_1 & E \\ i & j \end{pmatrix}\begin{matrix} E \\ k \end{matrix}\Big)=\begin{pmatrix} 1 & 0 \\ 0 & 1 \end{pmatrix},$$

$$\begin{pmatrix} E & A_2 \\ i & 1 \end{pmatrix}\begin{matrix} E \\ k \end{matrix}\Big)=\begin{pmatrix} A_2 & E \\ 1 & j \end{pmatrix}\begin{matrix} E \\ k \end{matrix}\Big)=\begin{pmatrix} 0 & 1 \\ -1 & 0 \end{pmatrix},$$

$$\begin{pmatrix} E & E \\ i & j \end{pmatrix}\begin{matrix} A_1 \\ 1 \end{matrix}\Big)=\frac{1}{\sqrt{2}}\begin{pmatrix} 1 & 0 \\ 0 & 1 \end{pmatrix},$$

$$\begin{pmatrix} E & E \\ i & j \end{pmatrix}\begin{matrix} E \\ 1 \end{matrix}\Big)=\frac{1}{\sqrt{2}}\begin{pmatrix} 1 & 0 \\ 0 & -1 \end{pmatrix},$$

$$\begin{pmatrix} E & E \\ i & j \end{pmatrix}\begin{matrix} A_2 \\ 1 \end{matrix}\Big)=\frac{1}{\sqrt{2}}\begin{pmatrix} 0 & 1 \\ -1 & 0 \end{pmatrix},$$

$$\begin{pmatrix} E & E \\ i & j \end{pmatrix}\begin{matrix} E \\ 2 \end{matrix}\Big)=\frac{1}{\sqrt{2}}\begin{pmatrix} 0 & -1 \\ -1 & 0 \end{pmatrix}.$$

The meaning of the symbols for the Clebsch-Gordan coefficients merits explanation. The representation of the total wave function of interest is written in the right half of the symbol. For example, $\left(\begin{smallmatrix} E & E \\ i & j \end{smallmatrix}\middle|\begin{smallmatrix} A_2 \\ 1 \end{smallmatrix}\right)$ specifies a coefficient for the total wave function Ψ^{A_2}, which transforms as (the one and only component of) A_2. The left-hand side of the symbol specifies the product states $\phi^{E_i}v^{E_j}$, from which it is constructed. The coefficient $\left(\begin{smallmatrix} E & E \\ i & j \end{smallmatrix}\middle|\begin{smallmatrix} A_2 \\ 1 \end{smallmatrix}\right)$ therefore specifies the decomposition of Ψ^{A_2} into products of basis states ϕ and v, both of which have E symmetry.

The indices i, j, and k in (A2) can each take on values 1 or 2, corresponding to X or Y, respectively. However, the indices i and j perform two functions: they specify rows and columns, respectively, in the symbol matrix, as well as basis-state representations. The index k specifies only X or Y for the degenerate representation of the total wave function. Further discussion in the context of the example above helps to clarify this point.

Prior to specifying ij index values in the symbol $\left(\begin{smallmatrix} E & E \\ i & j \end{smallmatrix}\middle|\begin{smallmatrix} A_2 \\ l \end{smallmatrix}\right)$, there are four possible combinations of $\phi^{E_i}v^{E_j}$ states which can contribute $(\Psi^{A_2})_{ij}$ terms to the total wave function Ψ^{A_2}. Using the matrices in (A2), contributions to total wave functions from any basis-state combination can be written down directly. In the example above, the explicit decomposition of Ψ^{A_2}, in terms of basis states of E symmetry, yields the following $(\Psi^{A_2})_{ij}$ terms:

$$(\Psi^{A_2})_{11}=0,$$

$$(\Psi^{A_2})_{12}=\frac{1}{\sqrt{2}}\,\phi^{E_X}v^{E_Y},$$

$$(\Psi^{A_2})_{21}=-\frac{1}{\sqrt{2}}\,\phi^{E_Y}v^{E_X},$$

$$(\Psi^{A_2})_{22}=0.$$

Other basis states may also make contributions to Ψ^{A_2}. Consequently, any complete, irreducible representation of the total wave function, such as those in (22) and (36), must sum over all basis states.

*Present address: OSRAM SYLVANIA INC., Lighting Research Center, 71 Cherry Hill Drive, Beverly, MA 01915.
[1] L. duPreez, Ph.D. dissertation, University of Witwatersrand, 1965.
[2] G. Davies and M. F. Hamer, Proc. R. Soc. London Ser. A **348**, 285 (1976).
[3] J. H. N. Loubser and J. P. van Wyk, *Diamond Research (London)* (Industrial Diamond Information Bureau, London, 1977), pp. 11–15.
[4] A. T. Collins, J. Phys. C **16**, 2177 (1983).
[5] N. B. Manson, X.-F. He, and P. T. H. Fisk, Opt. Lett. **15**, 1094 (1990).
[6] E. van Oort, N. B. Manson, and M. Glasbeek, J. Phys. C **21**, 4385 (1988); I. Hiromitsu, J. Westra, and M. Glasbeek, Phys. Rev. B **46**, 10 600 (1992).
[7] D. A. Redman, S. Brown, R. H. Sands, and S. C. Rand, Phys. Rev. Lett. **67**, 3420 (1991).
[8] N. R. S. Reddy, N. B. Manson, and E. R. Krausz, J. Lumin. **38**, 46 (1987).
[9] K. Holliday, N. B. Manson, M. Glasbeek, and E. van Oort, J. Phys. Condens. Matter **1**, 7093 (1989).
[10] D. A. Redman, S. W. Brown, and S. C. Rand, J. Opt. Soc. Am. B **9**, 768 (1992).
[11] A. Lenef, S. W. Brown, D. A. Redman, J. Shigley, E. Fritsch, and S. C. Rand, preceding paper, Phys. Rev. B **53**, 13 427 (1996).
[12] N. B. Manson, P. T. H. Fisk, and X.-F. He, Appl. Magn. Reson. **3**, 999 (1992).
[13] W. B. Fowler, *The Physics of Color Centers* (Academic, New York, 1968).
[14] C. A. Coulson and M. J. Kearsley, Proc. R. Soc. London Ser. A **241**, 433 (1957).
[15] M. Tinkham, *Group Theory and Quantum Mechanics* (McGraw-Hill, New York, 1964).
[16] See, for example, C. Cohen-Tannoudji *et al.*, *Quantum Mechanics* (Wiley, New York, 1977), Vol. II, p. 1215.
[17] A. Abragam and B. Bleaney, *Electron Paramagnetic Resonance of Transition Ions* (Clarendon, Oxford, 1970).
[18] A. Lenef, Ph.D. dissertation, University of Michigan, 1993.
[19] E. van Oort, B. van der Kamp, R. Sitters, and M. Glasbeek, J. Lumin. **48 & 49**, 803 (1991).
[20] H. A. Jahn and E. Teller, Proc. R. Soc. London Ser. A **161**, 220 (1937).
[21] J. Bourgoin and M. Lannoo, *Point Defects in Semiconductors II* (Springer Verlag, New York, 1983), Chap. 1.
[22] W. Ludwig and C. Falter, *Symmetries in Physics* (Springer-Verlag, New York, 1987).
[23] G. Davies, Rep. Prog. Phys. **44**, 787 (1981).